Riv. Mat. Univ. Parma (7) **8** (2008), 69-97

MARCO SECONDINI and Enrico FORESTIERI (*)

The nonlinear Schrödinger equation in fiber-optic systems (**)

1 - Introduction

This paper aims at providing an overview of the main themes related to the nonlinear Schrödinger equation (NLSE) in fiber-optic systems, with special attention to those aspects pertaining to communication theory. The NLSE for the propagation of light in *single-mode* optical fibers, in the presence of attenuation, dispersion, and nonlinear effects, was first derived in [**17**]. Its derivation from Maxwell's equations relies on some assumptions that are commonly met in today's fiber-optic communication systems [**1**]. Therefore, we take the NLSE as the starting point to derive suitable models for the fiber-optic channel. The analysis focuses on long-haul and ultra-long-haul systems, deploying *single-mode* fibers and optical amplifiers. The major simplification that will be made consists in neglecting polarization effects.

Although exact solutions of the NLSE are typically not known in analytical form, except for some specific cases in which the inverse scattering method can be applied [**42**], a large number of numerical methods have been proposed for its solution. Probably, the most known and widely adopted is the *split-step Fourier method* (SSFM) [**1, 3, 10, 12, 16, 17, 37, 39**], by which the propagation problem for a deterministic signal can be solved with arbitrarily high accuracy.

However, the signal waveform in a digital communication system depends on the random information sequence to be transmitted and is corrupted by noise.

(*) Scuola Superiore Sant'Anna - Via Moruzzi 1 - 56124 Pisa, Italy - marco.secondini@sssup.it

(**) Received 27th February 2008 and in revised form 24th April 2008. AMS classification: Primary 35Q55; Secondary 94A05, 94A40.

Therefore, the analysis of a fiber-optic system requires to consider the optical signal propagating through the fiber as the realization of a stochastic process, whose statistical properties — e.g., its probability density function (pdf) and power spectral density (PSD) — determine the average performance of the system.

An easy approach to the solution is provided by the Monte Carlo (MC) method, where the required statistical properties are estimated by averaging a large number of realizations. The MC method turns the stochastic problem into many deterministic problems, whose solutions can be numerically found by the SSFM. To reduce the number of required realizations, advanced simulation techniques have been proposed, such as importance sampling [**38**] or multicanonical Monte Carlo (MMC) [**13, 22**]. The accuracy of MC and other simulation methods can be increased at will by increasing the number of realizations. However, the computational cost for complex systems can still be extremely high. An alternative approach is the analytical evaluation of the required statistical properties by using simplified channel models [**2, 4, 5, 8, 9, 21, 24, 28, 29, 33-36**].

In this paper, after a short discussion on the SSFM and MC methods, we focus on the application of perturbation theory to the NLSE. As regards the deterministic problem, we derive two recursive expressions, based on a regular perturbation (RP) and a logarithmic perturbation (LP), that, starting from the linear solution, converge to the exact solution of the NLSE. As regards the stochastic problem, we investigate signal-noise interaction during propagation and review some perturbation methods for evaluating the pdf and PSD of the output signal, namely, the continuous wave (CW) approximation, that is based on a linearized RP expansion and neglects signal modulation [**5, 24, 26**], the more accurate covariance matrix method (CMM), that accounts for signal modulation and adopts a more robust linearization procedure [**21**], and the combined regular-logarithmic perturbation (CRLP), that is based on a different expansion — a combination of the RP and LP expansions — and accounts for the non-Gaussian distribution of the output signal [**33**]. We discuss the characteristics and limitations of the various methods and compare their accuracy. Finally, we highlight the issues still open to investigation.

The paper is organized as follows. Section 2 gives a basic overview of the main elements of a fiber-optic communication system. Section 3 reports the NLSE that governs the propagation of light in optical fibers and derives an alternative integral expression. Section 4 is dedicated to the propagation of a deterministic signal through the fiber, investigating different propagation regimes and comparing some numerical or perturbation approaches to this problem. Section 5 is dedicated to the propagation of a stochastic process through the fiber; again, different propagation regimes are investigated and some numerical or perturbation approaches are introduced and compared. Finally, Section 6 draws the conclusions.

2 - Fiber-optic systems

The main elements of a generic *long-haul* or *ultra long-haul* fiber-optic system are schematically depicted in Fig. 1. A composite optical signal is generated at the transmit end by modulating N lasers according to the information symbols from different sources. The lasers oscillate at different frequencies, appropriately spaced such that to avoid spectral overlap between channels. In this way, several signals are transmitted at different wavelengths on the same fiber, a technique referred to as *wavelength division multiplexing* (WDM).

The composite signal is then coupled to the optical fiber and propagates up to the receiver. In order to overcome the fiber loss and reach the desired distance, the signal has to be periodically amplified. Thus, the link is made of several spans of fiber interleaved by optical amplifiers.

At the receive end, each component signal is recovered by optical filtering, photodetected, filtered again in the electrical domain, and sampled. Finally, the information symbols are recovered from the output samples through a proper decision strategy. Different modulation formats can be adopted to carry the information, such as amplitude or phase modulations, using either binary or multilevel symbols. The most common format in current fiber-optic systems is *on-off keying* (OOK), a binary amplitude modulation format where "1's" are carried by marks (signal is on), and "0's" are carried by spaces (signal is off). The corresponding transmitted signal is represented as a *pulse amplitude modulation* (PAM) signal [**31**]

$$x(t) = \sum_k a_k p(t - kT_b), \tag{1}$$

where $\{a_k\}$ is a random sequence of independent bits taking on values 0 or 1 with equal probability, $p(t)$ is the elementary pulse, and $T_b = 1/R_b$ is the bit-time, that is

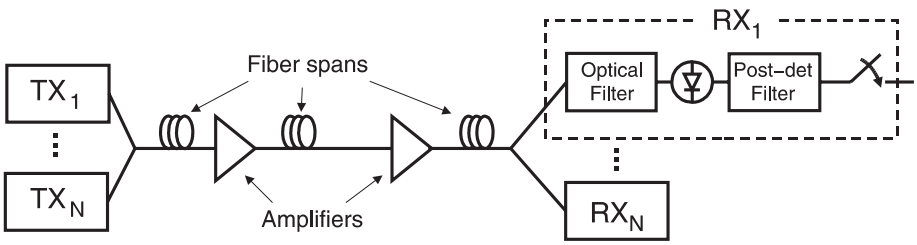

Fig. 1. Schematic representation of a *long-haul* or *ultra long-haul* fiber-optic communication system.

the inverse of the bit-rate R_b at which bits are transmitted. The signal in (1) is a representation of the actual transmitted signal $x_{\mathrm{bp}}(t)$, and their relation, assuming an ideal modulator and neglecting the phase noise of the laser source, is [1]

$$
\begin{aligned}
x_{\mathrm{bp}}(t) &= \Re\{x(t)\exp(j\omega_c t)\} \\
&= |x(t)|\cos\big[\omega_c t + \arg\big(x(t)\big)\big]
\end{aligned}
\tag{2}
$$

where $\omega_c = 2\pi f_c$, f_c being the oscillation frequency of the laser (the *carrier* frequency). As evident from (2), the modulus of $x(t)$ in (1) represents the amplitude modulation of $x_{\mathrm{bp}}(t)$, and its phase the corresponding phase modulation. The spectrum (i.e., the Fourier transform) of $x_{\mathrm{bp}}(t)$ is centered around f_c (which is in the order of 10^{14} Hz), whereas the spectrum of $x(t)$ is centered around 0 Hz. It is for this reason that $x(t)$ is said the *low-pass* equivalent of $x_{\mathrm{bp}}(t)$, which is *band-pass* in nature. Often, $x(t) = x_r(t) + jx_i(t)$ is also referred to as the *complex envelope* of $x_{\mathrm{bp}}(t)$, and its real $x_r(t)$ and imaginary $x_i(t)$ part as the in-phase and quadrature component, respectively.

Among all other modulations formats, the most interesting for fiber-optic systems are *differential phase-shift keying* (DPSK) and *differential quadrature-phase-shift keying* (DQPSK), a binary and quaternary (two bits per symbol) differential phase modulation format, respectively. Their low-pass equivalent signals are still as in (1), but the a_k symbols assume different values (they are complex valued in the DQPSK case).

At the transmit end, an optoelectronic modulator modulates the optical field at the input of the fiber according to the mathematical relation (2), such that the PAM signal (1) is the complex envelope of the transmitted signal, as already said. At the receive end, different optoelectronic front-ends are adopted according to the modulation format. In OOK systems, direct detection is usually used, as illustrated in Fig. 1. The photodetected current is then proportional to the intensity of the optical field and insensitive to its phase. Such systems are also known as *intensity-modulated direct-detection* (IMDD) systems. In DPSK and DQPSK systems, differential detection is usually adopted for the sake of retrieving the required phase information from the output optical signal without using a reference local oscillator.

Finally, coherent detection, based on the beating of the output optical signal with a local oscillator, is now being reconsidered [2] for next generation systems. In this

---

[1] As commonly done in the communication theory field, we denote by j the imaginary unit.

[2] Coherent detection has been rapidly replaced by direct detection after the introduction of optical amplifiers.

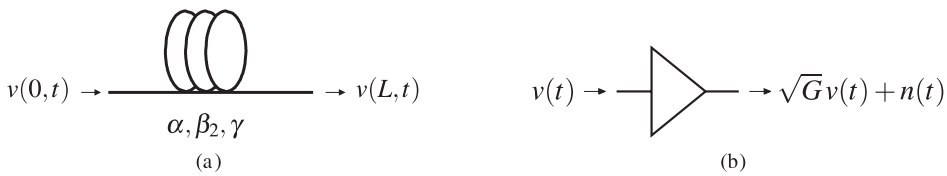

Fig. 2. (a) A generic fiber span of length L, with attenuation constant a, dispersion coefficient β_2, and nonlinear parameter γ. (b) An optical amplifier with power gain G and additive noise $n(t)$.

case, the photodetected current is proportional to the complex envelope of the optical field (two output currents proportional to the in-phase and quadrature components).

The basic elements of an optical link, i.e., a fiber span and an optical amplifier, are depicted in Fig. 2(a) and 2(b), respectively. Each span is characterized by its length L and by the fiber coefficients a, β_2, and γ [**1**], as explained in the following.

The attenuation constant a accounts for the exponential attenuation of the signal power during propagation caused by fiber loss; in standard fibers, its minimum value is $a \simeq 0.2\,\mathrm{dB/km}$ at a wavelength $\lambda = 1.55\,\mu\mathrm{m}$.

The parameter β_2 is equal to the second-order derivative with respect to frequency of the fiber mode-propagation constant β. The propagation constant β, whose frequency dependence is responsible for chromatic dispersion, can be expanded in Taylor series about the carrier frequency ω_c. The zeroth- and first-order coefficients of this expansion, β_0 and β_1, determine the absolute phase and propagation delay of the signal and are thus irrelevant, as they do not introduce distortions; the second-order coefficient $\beta_2 = \partial^2\beta/\partial\omega^2|_{\omega_c}$ accounts for *group velocity dispersion* (GVD) that causes pulse broadening during propagation; β_3 and higher-order coefficients account for third- and higher-order dispersion and can be usually neglected in single-channel systems. Commonly, the fiber chromatic dispersion is quantified through the so called dispersion parameter D, which is related to the GVD coefficient β_2 through the relation $D = -2\pi c\beta_2/\lambda_c^2$, where c is the speed of light and $\lambda_c = c/f_c$.

The parameter γ accounts for nonlinear refraction, that is the dependence of the refractive index on the intensity of the optical field (*Kerr* effect). It is related to the nonlinear-index coefficient n_2 and effective core area of the fiber A_{eff} through $\gamma = n_2\omega_c/(cA_{\mathrm{eff}})$ [**1**].

Both D and γ depends on the geometry of the fiber, which can be designed to obtain the desired characteristics. Typical values for standard single-mode fibers (SMF) at $\lambda = 1.55\,\mu\mathrm{m}$ are $D \simeq 17\,\mathrm{ps/(nm \cdot km)}$ and $\gamma \simeq 2\,\mathrm{W^{-1}/km}$. Other kind of fibers are also used for optical communications, characterized by a smaller or negative D and a higher γ. In multi-span systems, the propagation parameters a, β_2, and γ change along the link. Often, each span is made of a transmission fiber and a piece of fiber having coefficient β_2 of opposite sign, in order to compensate for GVD.

In general, GVD and nonlinear effects distort the elementary pulses in (1), such that they broaden and overlap. As a consequence, the output optical signal at time $t = kT_b$ depends not only on the current symbol a_k, but also on some neighboring symbols. This *inter-symbol interference* (ISI) is responsible for performance degradation.

The optical amplifiers, inserted in-line in order to recover the fiber loss, are usually modeled as a simple power gain G, followed by the addition of *amplified spontaneous emission* (ASE) noise. ASE noise can be modeled as *additive white Gaussian noise* (AWGN), with power spectral density $N_0 = (G-1)\eta_{\text{sp}}h\nu$, where $h\nu$ is the photon energy associated to the transition of an atom from the excited state to the normal state, and $\eta_{\text{sp}} = (N_2 - N_1)/N_1 \geq 1$ is the spontaneous emission coefficient that depends on the number of atoms N_2 and N_1 in those states.

Polarization mode dispersion (PMD), another relevant linear propagation effect in modern communication systems, will not be addressed in this paper.

3 - The nonlinear Schrödinger equation

The propagation of light in optical fibers is governed by the nonlinear Schrödinger equation (NLSE) and its variants [**1, 17**]. Neglecting polarization effects, and accounting for chromatic dispersion, nonlinear Kerr effect, and loss, in a time frame moving with the signal group velocity, the NLSE for a fiber span as that in Fig. 2 can be written as

$$\frac{\partial v}{\partial z} = j\frac{\beta_2}{2}\frac{\partial^2 v}{\partial t^2} - j\gamma|v|^2 v - \frac{a}{2}v, \tag{3}$$

where $v(z,t)$ is the optical field complex envelope, and a, β_2, and γ have been defined in the previous section. By letting $v(z,t) \triangleq \exp(-az/2)u(z,t)$, we can get rid of the last term in (3), which becomes

$$\frac{\partial u}{\partial z} = j\frac{\beta_2}{2}\frac{\partial^2 u}{\partial t^2} - j\gamma\exp(-az)|u|^2 u. \tag{4}$$

We note that in (4) the role played by the time and space variables, t and z, is exchanged with respect to the formulation of the NLSE used in quantum mechanics. In fact, (4) describes the spatial propagation along z of a waveform that is a function of time t. An alternative integral expression for the NLSE can be obtained as follows.

Letting

$$f(z,t) \triangleq e^{-az}|u(z,t)|^2 u(z,t) \tag{5}$$

and taking the Fourier transform[3] of (4), we obtain

$$\frac{\partial U}{\partial z} = -j\,\frac{\beta_2}{2}\omega^2 U - j\gamma F\,, \tag{6}$$

which, by the position

$$U(z,\omega) \triangleq e^{-j\beta_2\omega^2 z/2} Y(z,\omega)\,, \tag{7}$$

becomes

$$\frac{\partial Y}{\partial z} = -j\gamma e^{j\beta_2\omega^2 z/2} F\,. \tag{8}$$

Now, integrating (8) from 0 to z leads to

$$Y(z,\omega) = Y(0,\omega) - j\gamma \int_0^z e^{j\beta_2\omega^2\zeta/2} F(\zeta,\omega)\,d\zeta\,, \tag{9}$$

and, taking into account (7), we have

$$U(z,\omega) = U_0(z,\omega) - j\gamma \int_0^z e^{-j\beta_2\omega^2(z-\zeta)/2} F(\zeta,\omega)\,d\zeta\,, \tag{10}$$

where $U_0(z,\omega) = U(0,\omega)e^{-j\beta_2\omega^2 z/2}$ is the Fourier transform of the solution of (4) for $\gamma = 0$. Letting $H(z,\omega) \triangleq \exp(-j\beta_2\omega^2 z/2)$, so that $h(z,t) = \mathcal{F}^{-1}\{H(z,\omega)\}$, and inverse transforming (10) by taking into account (5), gives

$$u(z,t) = u_0(z,t) - j\gamma \int_0^z \Big[|u(\zeta,t)|^2 u(\zeta,t)\Big] \otimes h(z-\zeta,t)e^{-\alpha\zeta}\,d\zeta \tag{11}$$

where $\otimes$ denotes temporal convolution, defined as[4]

$$x(t) \otimes y(t) = \int_{-\infty}^{+\infty} x(t-\tau)y(\tau)\,d\tau\,, \tag{12}$$

and $u_0(z,t) = u(0,t) \otimes h(z,t)$ is the signal at z in a linear and lossless fiber.

---

[3] The Fourier transform with respect to time t of a function $x(z,t)$ is denoted by the same but capital letter $X(z,\omega)$, such that $X(z,\omega) = \mathcal{F}\{x(z,t)\}$, and $x(z,t) = \mathcal{F}^{-1}\{X(z,\omega)\}$, where $\mathcal{F}$ is the transform operator. A vector is denoted by a boldface letter $\boldsymbol{x}$ and its Fourier transform by the same boldface but capital letter $\boldsymbol{X}$.

[4] As evident, $x(t) \otimes y(t) = y(t) \otimes x(t)$ and we recall that $\mathcal{F}\{x(t) \otimes y(t)\} = X(f)Y(f)$.

Two different problems are usually considered. The first one is the propagation of a deterministic signal through the fiber, i.e., given the initial condition $u(0,t)$ for $t \in [-\infty, \infty)$, that is the optical field at the input of the fiber, one has to find the solution $u(z,t)$ at the output of the fiber. The second one is the propagation of a stochastic process through the fiber, i.e., given the statistical description of the input process $u(0,t)$, one has to find the statistical description of the output process $u(z,t)$. This last one is a typical problem in communication theory and is related to the stochastic nature of information symbols and noise. Most often, rather than in the full statistics of the output field $u(z,t)$, we are interested in the system error probability, which is directly related to the pdf of the photodetected signal, which, in turn, is related to the pdf and PSD of the optical signal. In this case, also the receiver structure plays a fundamental role in the definition of the stochastic problem.

4 - Deterministic problem

4.1 - *Dispersion-dominant regime*

When the nonlinear term of the NLSE is negligible, that is when $\gamma P_0 L \ll 1$, where P_0 is the peak input power and L the fiber length, (4) reduces to

$$\frac{\partial u}{\partial z} = j\,\frac{\beta_2}{2}\frac{\partial^2 u}{\partial t^2} \tag{13}$$

describing the signal evolution in the dispersion-dominant propagation regime, also known as linear propagation regime. In this case, practically achieved for low signal power, the fiber behaves as a linear dispersive system. The solution of (13) is readily found by taking the Fourier transform of both sides. Indeed, recalling that $\mathcal{F}\{d^n x(t)/dt^n\} = (j\omega)^n X(\omega)$, in the frequency domain (13) turns into a first order differential equation in z, whose solution is

$$U(z,\omega) = H(z,\omega)U(0,\omega) \tag{14}$$

where

$$H(z,\omega) = \exp\left(-j\,\frac{\beta_2}{2}\omega^2 z\right) \tag{15}$$

is the transfer function of the fiber, with unitary amplitude and parabolic phase. It is this parabolic phase due to GVD that causes pulse broadening during propagation along the fiber.

4.2 - *Nonlinearity-dominant regime*

When the linear term of the NLSE is negligible, that is when $\beta_2 B^2 L \ll 1$, B being the signal bandwidth, (4) reduces to

$$\frac{\partial u}{\partial z} = -j\gamma \exp(-\alpha z)|u|^2 u. \tag{16}$$

In this case, practically achieved for very low dispersion such as in zero-dispersion fibers, the fiber behaves as an instantaneous nonlinear system. The solution of (16) in the temporal domain is

$$u(z,t) = |u(0,t)| \exp\left(-j\gamma |u(0,t)|^2 L_{\text{eff}}\right) \tag{17}$$

showing that the signal undergoes a phase shift proportional to its intensity, while its amplitude does not change. This phenomenon is known as *self-phase modulation* (SPM) and the quantity $L_{\text{eff}} = [1 - \exp(-\alpha L)]/\alpha$ plays the role of an effective length, smaller than L because of fiber losses.

4.3 - *Split-step Fourier method*

In general, both the linear and nonlinear term of the NLSE are present and some numerical methods must be adopted to solve (4). Among the many methods devised to this aim, the SSFM is probably the most known and commonly used one in fiber-optic communications due to its simplicity and computational efficiency [**1, 3, 10, 12, 16, 17, 37, 39**].

The main idea behind SSFM is that, for a short propagation distance, dispersion and nonlinearity, in general acting together along the fiber, can instead be separated as if they act independently from each other. In its simplest formulation, the propagation over a small distance Δz is carried out in two steps. In the first step, (14) is used to propagate the signal as if dispersion was acting alone. In the second step, (17) is used to propagate the signal as if nonlinearity was acting alone. Since (14) and (17) are defined in the frequency and time domain, respectively, direct and inverse Fourier transforms must be performed at each step. This method takes advantage of the highly efficient implementation of the discrete Fourier transform through the fast Fourier transform (FFT) algorithm, and turns out to be faster than finite differences methods in most practical cases [**39**].

The complexity and accuracy of the SSFM is determined by three parameters, namely the time-width T and bandwidth B of the signal to be propagated, and the step-size Δz. Due to the periodic time and frequency boundary conditions implied by the discrete Fourier transform, some care must be taken in the choice of T and B.

Usually, although signals may be not strictly time- or band-limited, T and B are chosen wide enough such that almost all of the signal energy remains confined during propagation. In some cases, the signal is not time-limited but consists of an infinite aperiodic sequence of pulses, like in (1). However, as explained in the next Section, all the relevant propagation effects are correctly reproduced when replacing it with the periodic signal obtained by using a proper *pseudo-random bit sequence* (PRBS).

The signal is then represented over a single period $T = NT_b$, depending on the PRBS length N, and is assumed to be periodic in time (as required by the FFT algorithm) in order to exploit the cyclic properties of the PRBS. Once T and B have been fixed, the accuracy of the method depends on the step-size Δz. It has been demonstrated that the error due to a step-size Δz is of second-order in Δz for the simplest SSFM formulation described above, while reducing to third-order for the symmetric SSFM, obtained by dividing the linear propagation in two half-steps and applying the nonlinearity in the middle [**10**]. This fact ensures the convergence of the method and allows to obtain an arbitrarily high accuracy by simply reducing Δz. In particular, for a given accuracy, the required step-size depends on the inter-play between dispersion and nonlinearity along the fiber, that is on the signal bandwidth and power and on the fiber dispersion and nonlinear parameters. In practice, the step-size can be fixed according to some guide-lines [**12**], can be iteratively reduced until the changes in the output signal are within the desired accuracy, or can be adaptively adjusted along the propagation [**3, 37**].

The overall complexity, which any other alternative numerical method should be compared to, is determined by the number and size of FFTs to be performed. The product BT determines the number of complex numbers required to represent the signal, that is the size of each FFT. The step-size Δz determines the total number of steps, that is the number of direct and inverse FFTs to be performed.

4.4 - *Perturbation methods*

An alternative approach to the solution of (4) is based on perturbation theory. The idea is that of expressing the signal $u(z,t)$ as a power series in the nonlinear coefficient γ. The leading term of this power series is the linear solution (14) for $\gamma = 0$, while further terms describe the deviation from the linear solution due to nonlinearity and are obtained recursively. Here we present two recursive expressions that, starting from the linear propagation solution, asymptotically converge to the exact solution. The first one corresponds to the well-known RP method, whereas the second one corresponds to an LP method, and constitutes an all-order generalization of the first-order multiplicative approximation in [**9**].

4.4.1 - Regular perturbation

According to the RP method [**41**], expanding the optical field complex envelope $u(z,t)$ in power series in γ

$$u(z,t) = \sum_{k=0}^{\infty} \gamma^k u_k(z,t) \tag{18}$$

and substituting (18) in (11), after some algebra we obtain

$$\sum_{k=1}^{\infty} \gamma^k u_k = \sum_{n=0}^{\infty} \gamma^{n+1} \left[-j \int_0^z \left(\sum_{k=0}^{n} \sum_{i=0}^{k} u_i u_{k-i} u_{n-k}^* \right) \otimes h(z-\zeta,t) e^{-\alpha\zeta} d\zeta \right], \tag{19}$$

where we omitted the arguments (z,t) for the u_k's appearing on the left side, and (ζ,t) for those on the right side. By equating the powers in γ with the same exponent, we can recursively evaluate all the u_k's

$$u_n = -j \int_0^z \left(\sum_{k=0}^{n-1} \sum_{i=0}^{k} u_i u_{k-i} u_{n-k}^* \right) \otimes h(z-\zeta,t) e^{-\alpha\zeta} d\zeta\,, \quad n \geq 1\,. \tag{20}$$

As an example, the first three u_k's are

$$u_1 = -j \int_0^z \left(|u_0|^2 u_0 \right) \otimes h(z-\zeta,t) e^{-\alpha\zeta} d\zeta\,,$$

$$u_2 = -j \int_0^z \left(2|u_0|^2 u_1 + u_0^2 u_1^* \right) \otimes h(z-\zeta,t) e^{-\alpha\zeta} d\zeta\,,$$

$$u_3 = -j \int_0^z \left(2|u_0|^2 u_2 + u_0^2 u_2^* + 2|u_1|^2 u_0 + u_1^2 u_0^* \right) \otimes h(z-\zeta,t) e^{-\alpha\zeta} d\zeta\,.$$

Turning again our attention to (11), we note that it suggests the following recurrence relation

$$\begin{aligned} v_0(z,t) &= u_0(z,t) \\ v_{n+1}(z,t) &= u_0(z,t) - j\gamma \int_0^z \left[|v_n(\zeta,t)|^2 v_n(\zeta,t) \right] \otimes h(z-\zeta,t) e^{-\alpha\zeta} d\zeta \end{aligned} \tag{21}$$

and it is easy to see that

$$\lim_{n\to\infty} v_n(z,t) = u(z,t) \tag{22}$$

as it can be shown that

$$\frac{1}{k!}\frac{\partial^k v_n(z,t)}{\partial \gamma^k}\bigg|_{\gamma=0} = u_k(z,t), \qquad 0 \le k \le n\,. \tag{23}$$

This means that the rate of convergence of (21) is not greater than that of (18) when using the same number of terms as the recurrence steps, i.e., it is poor [**41**]. We will now seek an improved recurrence relation with an accelerated rate of convergence to the solution of (4).

4.4.2 - Logarithmic perturbation

As shown in [**9**], a faster convergence rate is obtained when expanding in power series in γ the log of $u(z,t)$ rather than $u(z,t)$ itself as done in (18). So, we recast (11) in terms of $\log u(z,t)$ and rewrite it as

$$\frac{u(z,t)-u_0(z,t)}{u_0(z,t)} = -\frac{j\gamma}{u_0(z,t)}\int_0^z \Big[|u(\zeta,t)|^2 u(\zeta,t)\Big] \otimes h(z-\zeta,t)e^{-a\zeta}d\zeta\,. \tag{24}$$

Using now the expansion

$$\log\frac{u}{u_0} = \frac{u-u_0}{u_0} - \frac{1}{2}\left(\frac{u-u_0}{u_0}\right)^2 + \frac{1}{3}\left(\frac{u-u_0}{u_0}\right)^3 - \dots \tag{25}$$

we replace the term $(u-u_0)/u_0$ in (24), obtaining

$$\log\frac{u}{u_0} = -\frac{j\gamma}{u_0}\int_0^z \Big[|u|^2 u\Big] \otimes h\, e^{-a\zeta}d\zeta - \frac{1}{2}\left(\frac{u-u_0}{u_0}\right)^2 + \frac{1}{3}\left(\frac{u-u_0}{u_0}\right)^3 - \dots \tag{26}$$

where, for simplicity, we omitted all the function arguments. So, the sought improved recurrence relation suggested by (26) is

$$\begin{aligned} v_0 &= u_0 \\ v_{n+1} &= v_n \exp\left\{-\frac{j\gamma}{v_0}\int_0^z \Big[|v_n|^2 v_n\Big] \otimes h(z-\zeta,t)e^{-a\zeta}d\zeta - \frac{v_n - v_0}{v_0}\right\} \end{aligned} \tag{27}$$

where we used again (25) to obtain the right side of the second equation. Also in this

case $\lim_{n\to\infty} v_n(z,t) = u(z,t)$, as it can be shown that the power series in γ of $\log v_n(z,t)$ coincides with that of $\log u(z,t)$ in the first n terms.

Notice that $v_1(z,t)$ evaluated from (27) coincides with the first-order multiplicative approximation in [**9**], there obtained with a different approach. The method in [**9**] is really an LP method as the solution $u(z,t)$ is written as

$$u(z,t) = u_0(z,t)e^{-j\gamma\vartheta(z,t)}, \quad \vartheta = \vartheta_0 + \gamma\vartheta_1 + \gamma^2\vartheta_2 + \dots \tag{28}$$

and $\vartheta_0(z,t)$, $\vartheta_1(z,t)$ are evaluated by analytically approximating the SSFM solution. The calculation of $\vartheta_n(z,t)$ becomes progressively more involved for increasing values of n, but that method is useful because it can provide an analytical expression for the SSFM errors due to a finite step size [**9**].

We now follow another approach. Letting

$$\psi_n(z,t) \triangleq -j\vartheta_{n-1}(z,t)\,, \tag{29}$$

such that

$$u(z,t) = u_0(z,t)\exp\big(\gamma\psi_1(z,t) + \gamma^2\psi_2(z,t) + \gamma^3\psi_3(z,t) + \dots\big), \tag{30}$$

for every n, $\psi_n(z,t)$ can be easily evaluated in the following manner. The power series expansion of $u(z,t)$ in (30) is

$$\begin{aligned} u_0\exp\left(\sum_{k=1}^{\infty}\gamma^k\psi_k\right) &= u_0\sum_{i=0}^{\infty}\frac{1}{i!}\left(\sum_{k=1}^{\infty}\gamma^k\psi_k\right)^i \\ &= u_0\left[1 + \sum_{n=1}^{\infty}\left(\sum_{k=1}^{n}\frac{\varphi_{n,k}}{k!}\right)\gamma^n\right] \end{aligned} \tag{31}$$

where

$$\varphi_{n,k} = \begin{cases} 0 & \text{if } n \neq 0, k = 0 \\ 1 & \text{if } n = k = 0 \\ \displaystyle\sum_{m=k-1}^{n-1}\varphi_{m,k-1}\psi_{n-m} & \text{otherwise}\,. \end{cases} \tag{32}$$

Equating (18) to (31), and taking into account that $\varphi_{n,1} = \psi_n$, we can recursively evaluate the ψ_n's as

$$\psi_n = \frac{u_n}{u_0} - \sum_{k=2}^{n}\frac{\varphi_{n,k}}{k!}\,. \tag{33}$$

Thus, from the n-th order RP approximation we can construct the n-th order LP

approximation. As an example we have

$$\begin{aligned}
\psi_1 &= \frac{u_1}{u_0}\,, \\
\psi_2 &= \frac{u_2}{u_0} - \frac{1}{2}\psi_1^2\,, \\
\psi_3 &= \frac{u_3}{u_0} - \psi_1\psi_2 - \frac{1}{6}\psi_1^3\,, \\
\psi_4 &= \frac{u_4}{u_0} - \psi_1\psi_3 - \frac{1}{2}\psi_2^2 - \frac{1}{2}\psi_1^2\psi_2 - \frac{1}{24}\psi_1^4\,.
\end{aligned}$$

So, once evaluated the u_k's from (20), we can evaluate the ψ_k's from (33) and then $u(z,t)$ through (30), unless $u_0(z,t)$ is zero (or very small), in which case we simply use (18) as in this case $u(z,t)$ is also small and (18) is equally accurate.

The computational complexity of (20), (21) and (27) is the same, and at first glance it may seem that a n-th order integral must be computed for the n-th order approximation. However, it is not so and the complexity only increases linearly with n. Indeed, the terms depending on z can be taken out of the integration [5] and so all the integrals can be computed in parallel. However, only for $n \leq 2$ these methods turn out to be faster than the SSFM because of the possibility to exploit efficient quadrature rules for the outer integral, whereas the inner ones are to be evaluated through the trapezoidal rule as, to evaluate them in parallel, we are forced to use the nodes imposed by the outer quadrature rule. Nevertheless, for practical values of input power and number of spans, as those used in current dispersion managed systems, the second-order LP method can provide accurate results in a shorter time than the SSFM (we estimated an advantage of about 30% for approximately the same accuracy).

To illustrate the results obtainable by the RP and LP methods, Fig. 3 shows the output intensity for a single pulse transmitted through a 5×100 km link, composed of 5 spans of 100 km transmission fiber followed by a compensating fiber and per span amplification recovering all the span loss. The input signal is a rectangular 100-ps pulse, filtered by a Gaussian filter with bandwidth equal to 20 GHz, with a peak power of 12 dBm. The transmission fiber is a standard single-mode fiber with $\alpha = 0.19$ dB/km, $D = 17$ ps/nm/km, $\gamma = 1.3$ W^{-1}km^{-1}, whereas the compensating fiber has $\alpha = 0.6$ dB/km, $D = -100$ ps/nm/km, $\gamma = 5.5$ W^{-1}km^{-1}, and a length such that the residual dispersion per span is zero. The "exact" solution is obtained by the

[5] This is apparent when performing the integrals in the frequency domain, but is also true in the time domain as $h(z-\zeta,t) = h(z,t) \otimes h(-\zeta,t)$ when $h(\ell,t)$ is the impulse response of a linear fiber of length ℓ ($h(-\zeta,t)$ simply corresponds to a fiber of length ζ and opposite sign of dispersion parameter).

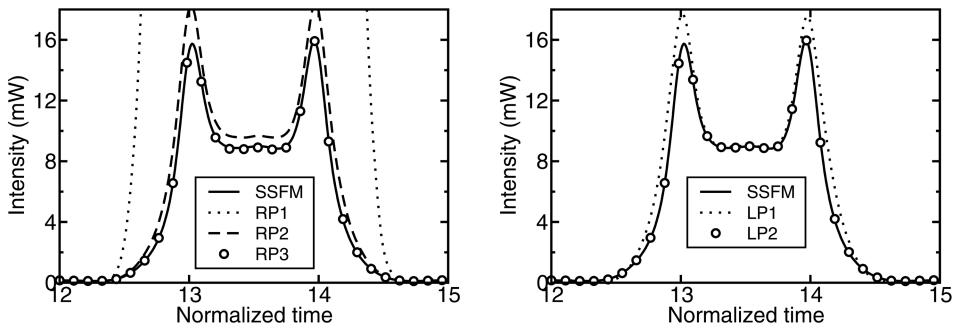

Fig. 3. Output intensity for a single pulse with $P_{in} = 12$ dBm and 5 spans.

SSFM with a step size of 100 m, while RPn and LPn are the n-th order solutions obtained by the RP and LP method, respectively.

In this case, 3rd-order is required to obtain an accurate result through the RP method, whereas only 2nd-order through the LP method.

5 - Stochastic problem

The stochastic problem consists in the propagation of a stochastic process through the fiber and the evaluation of its output statistics and system error probability. A first source of stochasticity is given by the random information symbols in (1) and a simple approach to account for it is that of replacing the random sequence with a deterministic periodic sequence having appropriate properties. For example, a binary de Bruijn sequence of order n — which is a cyclic sequence of 2^n bits where every possible subsequence of length n appears exactly once [**14**] — is one of such sequences. Considering a periodic signal corresponding to a de Bruijn sequence of order n, it is possible to account for ISI due to a maximum of n bits by averaging over the 2^n symbols. PRBSs of length $2^n - 1$, often used in experiments as they are easily obtainable through shift registers, have similar properties, but differ from de Bruijn sequences for a missing zero in the longest run of consecutive zeros. Most often, both sequences are called PRBS without distinction.

A second source of stochasticity is represented by the ASE noise introduced by optical amplifiers. Neglecting transient effects, which are usually treated separately, lumped optical amplifiers can be modeled as a signal power gain G, plus the addition of AWGN, at the points where the amplifiers are located. This is formally represented by adding a forcing term to the NLSE (4) and replacing the exponential attenuation term $\exp(-az)$ with a more general power-profile function $g(z)$ that

comprehends both the exponential attenuation and lumped gain G

$$\frac{\partial u}{\partial z} = j\,\frac{\beta_2}{2}\frac{\partial^2 u}{\partial t^2} - j\gamma g(z)|u|^2 u + w\,. \tag{34}$$

Here, the Langevin term is $w(z,t) \triangleq \sum_i n(z_i,t)\delta(z-z_i)$, where z_i is the location of the i-th amplifier, $\delta(z-z_i)$ the Dirac delta function, and the $n(z_i,t)$ are independent identically distributed complex Gaussian random processes with zero mean $E\{n(z_i,t)\} = 0$ and covariance function $E\{n(z_i,t)n^*(z_j,t+\tau)\} = N_0\delta(\tau)\delta_{ij}$, where δ_{ij} is the Kronecker delta function.

In WDM systems, also the neighboring channels are a source of stochasticity. Due to Kerr nonlinearity, these channels can affect the main channel by some effects like *four-wave mixing* (FWM) or *cross-phase modulation* (XPM) [**1**]. Since each channel carries a random sequence of information symbols, also these effects require a statistical description. According to the problem under investigation, different approaches can be followed to model FWM and XPM. They can be treated deterministically by using de Bruin sequences for all the channels, or can be approximated as additional noise sources (often Gaussian distributed) on the amplitude and phase of the signal [**2, 7, 28, 40**], or can be more accurately modeled by pulse-to-pulse interactions among the channels [**36**].

In this Section we describe different approaches to the stochastic problem, with a special attention to ASE noise and focusing on single-channel systems.

5.1 - *Dispersion-dominant regime*

When nonlinearities can be neglected, the NLSE reduces to (13) and the fiber behaves as a linear dispersive channel with transfer function (15). In this case, the linear superposition principle allows to independently solve the propagation problem for all the signals at different wavelengths and for the ASE noise. Therefore, each WDM channel is not affected by the presence of the other channels and can be modeled as a single-channel system. The signal propagation problem is easily solved by (14), while the ASE noise distribution is not affected by propagation. In fact, a Gaussian process remains Gaussian when passing through a linear system, while its power density spectrum gets multiplied by the squared modulus of the system transfer function [**6, 30**]. Since the transfer function (15) has a unitary modulus, the noise distribution is unchanged. This important property holds also when considering *polarization mode dispersion* (PMD) and implies that in linear systems, the ASE noise introduced by all the amplifiers along the line can be modeled as AWGN at the end of the line. This simple AWGN model is commonly adopted also in the presence of weak nonlinearities. In this case, nonlinear effects are included in the propagation of

the noise-free signal, that is numerically evaluated as explained in the previous section, but are neglected in the propagation of the ASE noise, that is still approximated as AWGN at the end of the link.

For coherent receiver, under the AWGN assumption, the final problem of error probability evaluation turns out to be the classical problem of communications through a linear AWGN channel and is widely treated in text books like [**31**]. On the other hand, for direct-detection receivers, by far the most widely deployed in today's systems, error probability evaluation is a quite complex problem also for the AWGN channel, due to the presence of the square-law detector. An accurate and efficient solution can be obtained by a time-domain [**25**], frequency-domain [**27**], or Fourier basis [**11**] Karhunen-Loève series expansion (KLSE) of the optical signal. First, the KLSE is used to found the moment generating function (MGF) of the photodetected sample. Then, the MGF is directly used for evaluating the bit-error probability through the *saddle-point* method [**18**].

5.2 - *Nonlinearity-dominant regime*

When the linear term is negligible, the NLSE reduces to (16) and has the explicit analytic solution (17). In this case, the fiber behaves as an instantaneous nonlinearity, implying that the process remains white during propagation, i.e., its samples are uncorrelated in time. However, its distribution changes. In particular, the interaction between amplifier noise and Kerr effect induces nonlinear phase noise — also known as Gordon-Mollenauer effect [**15**]. According to (17), the amplitude fluctuations on $|u(z,t)|$ due to ASE noise are directly converted into phase fluctuations by the Kerr effect. This has a significant impact on phase-modulated systems, whose maximum achievable distance is strongly reduced by nonlinear phase noise, while theoretically does not affect IMDD systems, that are sensitive only to the amplitude of the signal. An exact analysis of this case is given in [**29**]. Different approximations and simplified models are also discussed and compared in [**19**].

We note that the zero-dispersion regime is not practical for communications, since the absence of dispersion strongly enhances nonlinear effects, specially those related to the interactions among WDM channels, such as FWM and XPM. However, the theory developed for this simple case turns useful for the approximated analysis of WDM phase-modulated systems when both dispersion and nonlinearity are present [**20**].

5.3 - *Monte Carlo methods*

In the most general case, both dispersion and nonlinearities must be considered and the stochastic problem becomes hardly treatable by analytical methods. A

powerful tool for the statistical analysis of such complex systems is the Monte Carlo (MC) method. In its classical formulation, the MC method is a brute force method that turns the solution of the stochastic problem into the solution of many (from thousands to billions) deterministic problems. The problem is defined by the NLSE (34), and by the statistical description of the input signal $u(0,t)$ and of the Langevin term $w(z,t)$. Several independent realizations of all the stochastic quantities involved in the definition of the problem are drawn according to their known distributions. For each realization, the deterministic problem obtained by substituting the corresponding quantities in (34) is solved by a numerical method such as the SSFM. The desired statistical quantity — the output signal distribution or the error probability — is finally evaluated by averaging.

For instance, in a single-channel OOK system, the input optical signal $u(0,t)$ depends on the $N = T/T_b$ information bits, $a_1, \ldots, a_N$, in the time window T, while the forcing term $w(z,t)$ is represented by the $M = N_A B T$ independent Gaussian-distributed complex coefficients, $n_1, \ldots, n_M$, required to represent the ASE noise generated by N_A amplifiers on the timewidth T and bandwidth B. The expansion timewidth T and bandwidth B are chosen according to the system memory and bandwidth, as explained in Section 4.3. The distribution of the state vector $\boldsymbol{z} = [n_1, \ldots, n_M, a_1, \ldots, a_N]$ is then

$$p(\boldsymbol{z}) = \left(2\pi\sigma^2\right)^{-L/2} \prod_{m=1}^{M} \exp\left(-\frac{n_m^2}{2\sigma^2}\right) \cdot \prod_{k=1}^{N} \left[\frac{1}{2}\delta(a_k) + \frac{1}{2}\delta(a_k - 1)\right]. \tag{35}$$

The independent realizations of the random vector $\boldsymbol{z}$ are drawn by using standard routines for random number generation. The corresponding output signals are obtained by substituting the components of $\boldsymbol{z}$ into $u(0,t)$ and $w(z,t)$, and solving (34) by the SSFM, eventually including the receiver and the detection strategy. The desired output distribution is finally obtained by averaging. For instance, if we are interested in the bit-error probability, we can estimate it by the ratio between the number of errors at the receiver and the total number of transmitted bits. However, standard MC methods are not efficient in estimating low-probability events such as the error probability in a fiber-optic system, which can be as low as 10^{-12}. In this case, different techniques — e.g., importance sampling, Markov chain Monte Carlo, multicanonical Monte Carlo (MMC) — are available.

The first application of MMC to the solution of the problem described in this section was reported in [**22**]. The method was extended in [**13**] to exponentially increase the computational efficiency in long memory systems requiring a large expansion timewidth T. In principle, the extension of [**13**] to WDM systems is straightforward and could be done by including the information symbols of all the WDM channels in the state vector $\boldsymbol{z}$ and building the input signal $u(0,t)$ as the su-

perposition of all the signals transmitted at different wavelengths. However, the size of the problem increases rapidly with the number of channels, making also MMC practically unfeasible. Indeed, a larger bandwidth B is required to accommodate all the WDM channels, a larger T is required to account for the *walk-off* [**1**] between channels, and a smaller Δz is required for the SSFM because of the larger bandwidth and total power.

5.4 - *Perturbation methods*

An alternative approach to the stochastic problem is based again on perturbation theory. For instance, perturbation methods are suitable for investigating signal-noise interaction during propagation, where the noise can be considered as a small perturbation of the noise-free signal. Two typical effects induced by signal-noise interaction are parametric gain, that is the amplification of noise at some frequencies, and nonlinear phase noise, that is the phase noise generated by the conversion of the amplitude fluctuations due to ASE noise into phase fluctuations, as shown in (17). In the following, we shortly review the perturbation methods that have been proposed to account for signal-noise interaction and briefly introduce a novel perturbation method that we have recently proposed in [**33**], giving a unified description of nonlinear phase noise and parametric gain.

5.4.1 - The continuous wave approximation

The simplest approach to study parametric gain and its impact on system performance has been proposed in [**5, 24, 26**]. The idea is that, for the purpose of investigating the interaction between signal and noise, the signal can be approximated as the continuous wave (CW) solution of the NLSE, and the noise can be considered as a small perturbation of the CW and treated by the RP theory. The solution of the NLSE is written as

$$u(z,t) = \sqrt{P_0}[1 + c(z,t)] \exp\left[-j\phi_{\mathrm{NL}}(z)\right], \tag{36}$$

where P_0 is the power of the noise-free solution, $c(z,t) = a(z,t) + jb(z,t)$ is the additive perturbation, and

$$\phi_{\mathrm{NL}}(z) = \int_0^z \gamma P_0 \exp(-a\xi) d\xi \tag{37}$$

is the deterministic time-independent nonlinear phase rotation of the noise-free solution. Substituting (36) into (4), dropping all the terms that are nonlinear in c,

separating the real and imaginary parts, and finally taking the Fourier transform, we obtain a linear system of two differential equations

$$\begin{aligned} \frac{\partial A}{\partial z} &= \frac{\beta_2}{2}\omega^2 B, \\ \frac{\partial B}{\partial z} &= -\frac{\beta_2}{2}\omega^2 A - 2\gamma P_0 \exp(-az) A, \end{aligned} \tag{38}$$

whose solution can be expressed in matrix notation as $\boldsymbol{X}(z,\omega) = \mathbb{T}(z,\omega)\boldsymbol{X}(0,\omega)$, where $\boldsymbol{X} = [A,B]^T$ is the Fourier transform of the vector process $\boldsymbol{x} = [a,b]^T$ and $\mathbb{T}$ is the 2×2 transfer matrix for the RP model [6]. For constant fiber coefficients, in the absence of attenuation, the transfer matrix $\mathbb{T}$ has a simple closed-form expression [**24**]. In the presence of attenuation, $\mathbb{T}$ can be expressed either in terms of Hankel's functions of first and second kind [**5**], or calculated by dividing the fiber in several steps with negligible attenuation and multiplying the transfer matrices of each step [**24**]. Later, we will get back to the last approach, that can also be adopted for other perturbation methods and in the general case of a multi-span link. Now we consider a simple case, where the ASE noise is added to the CW at the input of the fiber and propagates through a single span according to (38). Thus, $\boldsymbol{x}(z,t)$ is a Gaussian vector process described by its PSD matrix

$$\mathbb{G}(z,\omega) \triangleq \Im_\tau\{E\{\boldsymbol{x}(z,t)\boldsymbol{x}^T(z,t+\tau)\}\}, \tag{39}$$

where $E\{\cdot\}$ denotes expectation and $\Im_\tau\{\cdot\}$ the Fourier transform with respect to τ. At the input of the fiber, the PSD matrix is $\mathbb{G}(0,\omega) = (N_0/2)\,\mathbb{I}$, with $\mathbb{I}$ the identity matrix. After propagation, the vector remains Gaussian and its PSD matrix becomes [**30**]

$$\mathbb{G}(z,\omega) = \mathbb{T}(z,\omega)\mathbb{G}(0,\omega)\mathbb{T}^T(z,\omega), \tag{40}$$

meaning that, in general, the output noise is not white and its in-phase and quadrature components are correlated. As anticipated, the in-phase component a can be subject to amplification or attenuation at certain frequencies, with a significant (positive or negative) impact on performance. In [**4**], the error probability is originally evaluated by a time-domain KLSE method, but in practice other KLSE methods [**11, 27**] can be easily extended to account for the colored noise.

The CW approximation is used only to determine the output PSD matrix of the noise, while the output noise-free signal, modulated by a PRBS, is evaluated by the SSFM. According to the CW approximation, the noise would remain stationary. However, a different PSD is evaluated for each bit a_k of the PRBS by using in (38) a

[6] A matrix is denoted by a capital blackboard letter such as $\mathbb{T}$.

CW power P_0 equal to the signal power at time $t = kT_b$ (in practice, parametric gain can be neglected when spaces are transmitted since P_0 is close to zero). Finally, the error probability is evaluated for each bit of the PRBS and averaged.

5.4.2 - The covariance matrix method

A more accurate approach to this problem has been later proposed in [**21, 23**] to overcome the strong limitations of the CW approximation. First, the authors remove the CW approximation by applying the RP theory to the modulated signal. The solution of the NLSE is written as $u(z,t) = u_0(z,t) + \delta u(z,t)$, where u_0 is the noise-free solution of the NLSE, numerically evaluated, and δu is the additive perturbation term. Substituting u into (4) and dropping all the terms that are nonlinear in δu, one obtain a linearized propagation equation for δu. Expanding both u_0 and δu in Fourier series with period equal to the PRBS period T, the equation is finally turned into a system of linear differential equations for the Fourier coefficients of δu.

Taking the ASE noise introduced by amplifiers as the input perturbation, the input variables are independent and identically distributed complex Gaussian variables, with zero mean and diagonal covariance matrix. In principle, considering the linearized system, the output coefficients should remain Gaussian and their covariance matrix could be evaluated by solving the system. Unfortunately, the linearization does not hold in many cases, meaning that the output coefficients are not Gaussian distributed and this simple procedure cannot be applied. Indeed, we have shown in Section IV that the main effect of Kerr nonlinearity is a phase rotation of the signal, that is poorly represented by a linear additive perturbation term. The solution proposed in [**21**] is that of extracting the phase- and time-jitter associated to each pulse of the PRBS. After jitter removal, the linearization of the NLSE is more robust and the output perturbation coefficients can be approximated as Gaussian.

Two different procedures for the evaluation of the covariance matrix of the perturbation coefficients, based on Monte Carlo simulations or on the Lyapunov method, are described in details in [**21**] and [**23**], respectively. From the covariance matrix, the error probability is finally evaluated by an extension of [**11**], as already discussed concerning the CW approximation. While the phase-jitter does not affect the performance of an IMDD system, time-jitter can be detrimental in highly nonlinear systems and must be included in the error probability evaluation. The accuracy of CMM is good also for highly nonlinear systems. However, it does not give a complete statistical characterization of the output process and its application is limited to IMDD systems and to the return-to-zero format. Moreover, some care must be taken when the signal pulses overlap during propagation.

5.4.3 - The combined regular-logarithmic perturbation

Finally, we shortly describe an alternative perturbation method that we have recently introduced in [**33**]. The idea is that the inaccuracy of the CW model is mainly due to the linearization rather than to the CW approximation. In fact, some works have already shown that a simple linearization does not hold in many cases [**21**], and second-order perturbation terms may not be neglected, since they can produce a strong degradation of the system performance [**34**]. As done in the CW approximation, we make the hypothesis that, for the purpose of investigating the interaction between signal and noise, the signal can be considered a continuous wave (CW), and the noise can be treated as a perturbation of the CW solution of the NLSE. The novelty of our approach is that in the place of the classical RP expansion (36), we write the perturbed solution of the NLSE as

$$u(z,t) = \sqrt{P_0}[1 + c(z,t)] \exp\{-j[\phi_{\mathrm{NL}}(z) + \phi(z,t)]\}. \tag{41}$$

Equation (41) is motivated by the evidence, given in Section 4.4, that the LP solution of the NLSE can be more accurate than the RP solution, but becomes singular when the signal power goes to zero. Therefore, it includes both the complex RP component $c(z,t) = a(z,t) + jb(z,t)$ and a real LP component $\phi(z,t)$. Equation (41) can also be regarded as a generalization and formalization of the phase-jitter removal concept introduced in the CMM [**21**], with the difference that in (41) the phase jitter is directly determined from the perturbed solution through the time-dependent term $\phi(z,t)$. Substituting (41) in (4), exploiting the additional degree of freedom given by the term ϕ, and neglecting terms that are nonlinear in a, b, or ϕ, we obtain a linearized system of three real differential equations for the CRLP model. Taking the Fourier transform we finally obtain the linear system

$$\frac{\partial A}{\partial z} = \frac{\beta_2}{2}\omega^2(B - \Phi), \tag{42a}$$

$$\frac{\partial B}{\partial z} = -\frac{\beta_2}{2}\omega^2 A, \tag{42b}$$

$$\frac{\partial \Phi}{\partial z} = 2\gamma P_0 \exp(-az) A, \tag{42c}$$

whose solution can be expressed in matrix notation as $\boldsymbol{X}(z,\omega) = \mathbb{T}(z,\omega)\boldsymbol{X}(0,\omega)$, where $\boldsymbol{X} = [A, B, \Phi]^T$ is the Fourier transform of the vector process $\boldsymbol{x} = [a, b, \phi]^T$ and $\mathbb{T}$ is the 3×3 transfer matrix for the CRLP model. For constant fiber coefficients, in the absence of attenuation, the transfer matrix $\mathbb{T}$ has a simple closed-form expression [**33**]. As in the RP case, $\boldsymbol{x}$ is a Gaussian vector process

that remains Gaussian during propagation through the linear system (41), with a PSD matrix that evolves as in (40). However, the signal itself, given by the nonlinear combination of a, b, and ϕ in (41), is not Gaussian-distributed in general. In other words, even if the overall process is not Gaussian, it is nevertheless fully described by three Gaussian processes and their PSD matrix. The slight increase in complexity with respect to the RP, brought by the use of a 3×3 rather than 2×2 PSD matrix, is compensated by a higher accuracy. In fact, as it is shown in [**32**], the term ϕ accounts for the quadratic perturbation terms that are neglected in the RP.

5.4.4 - Multi-span systems

For the generalization of the perturbation methods to multi-span systems it is convenient to consider the modified NLSE in (34). When deriving the CRLP equations (42), the complex forcing term $w(z,t)$ results in two real forcing terms in (42a) and (42b).

Considering the generic i-th span of length L_i represented in Fig. 4, with the amplifier located at z_i, the PSD matrix at the output of the amplifier is

$$\mathbb{G}\big(z_i^+,\omega\big) = \mathbb{G}\big(z_i^-,\omega\big) + \mathbb{G}_0, \tag{43}$$

where $\mathbb{G}_0 = \mathrm{diag}\{N_0/2, N_0/2, 0\}$. In general, the attenuation is not negligible and the fiber parameters may vary along the span. Thus, we divide the span into N short steps of length $\Delta z = L_i/N$, as depicted in Fig. 4. Each step has a negligible attenuation $a\Delta z \simeq 0$, constant dispersion, and an effective nonlinear coefficient $\gamma_n = \gamma \exp(-an\Delta z)[1 - \exp(-a\Delta z)]/a\Delta z$. At each step, the corresponding transfer matrix $\mathbb{T}_n(\Delta z, \omega)$ is evaluated in closed-form as in [**33**], and the overall transfer

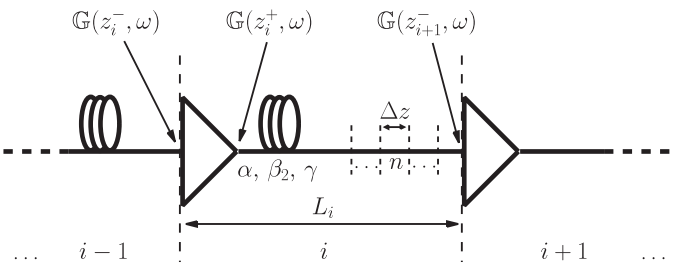

Fig. 4. Representation of the generic i-th span of a multi-span system with optical amplifiers. The span of length L_i, with variable parameters a, β_2, and γ is divided into N short steps of length $\Delta z = L_i/N$. Each step has constant values of the fiber parameters and negligible attenuation $a\Delta z \simeq 0$.

matrix is evaluated by multiplying all of them

$$\mathbb{T}(L_i, \omega) = \prod_{n=N}^{1} \mathbb{T}_n(\Delta z, \omega). \tag{44}$$

Finally, the PSD matrix at the output of the span is

$$\mathbb{G}\left(z_{i+1}^{-}, \omega\right) = \mathbb{T}(L_i, \omega)\mathbb{G}\left(z_i^{+}, \omega\right)\mathbb{T}^{T}(L_i, \omega). \tag{45}$$

By repeating the procedure described in (43)–(45) for each span composing the system, we finally obtain the output PSD matrix. As in the single-span case, the vector process $\boldsymbol{x}(z,t)$ remains Gaussian after propagation, while the signal $u(z,t)$ does not. The same procedure, described here for the CRLP, can be applied with minor modifications to the RP and CMM.

5.4.5 - Numerical comparison

Fig. 5 shows a comparison among the different methods presented here for the case of a CW signal plus AWGN noise propagating in a lossless fiber of length $L = 50\,\text{km}$, with nonlinear coefficient $\gamma = 2\,(\text{W}\cdot\text{km})^{-1}$. Such a simple case allows to focus only on the behavior and degree of accuracy of each method.

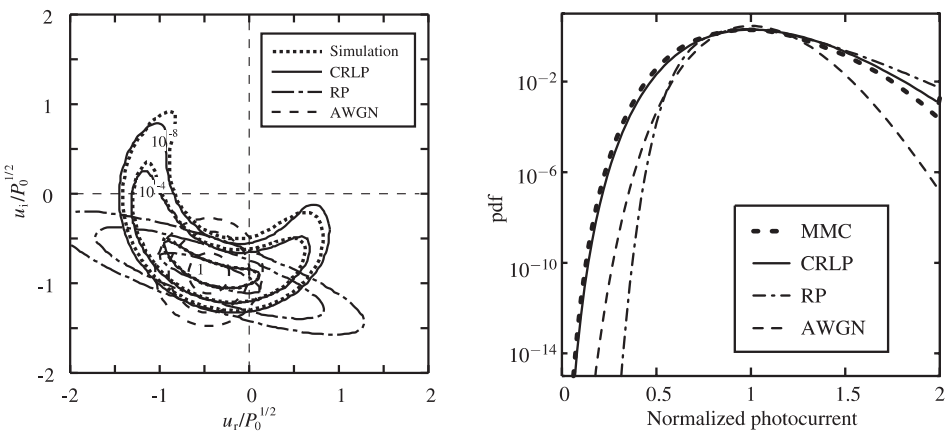

Fig. 5. - Comparison among the AWGN , RP, CRLP models, and MMC simulations for the propagation of a CW signal plus noise through a single lossless span: (a) joint pdf (level curves) of the real and imaginary parts of the output optical signal, $u = u_r + ju_i$, normalized to the square root of the CW power P_0; (b) pdf of the normalized photodetected current.

Fig. 5(a) reports the pdf of the optical signal after propagation. The CW power is $P_0 = 20\,\mathrm{mW}$, the noise PSD is $N_0 = 1.6 \cdot 10^{-14}\,\mathrm{W/Hz}$ — corresponding to an optical signal-to-noise ratio $\mathrm{OSNR}_{0.1\,\mathrm{nm}} \simeq 14\,\mathrm{dB}$ for an ideal 10 Gbit/s-NRZ signal with the same peak power — and the fiber has a normal dispersion $D = -5\,\mathrm{ps/(nm \cdot km)}$ (a reasonable value for non-zero dispersion fibers).

The contour lines of the joint pdf of the real and imaginary part of the normalized optical signal are reported for different levels and models. The dotted curves obtained by MMC simulations are taken as a reference, since they can be considered exact within the statistical uncertainty of the method. In this case, the large deviation of the MMC simulations from the AWGN model shows that signal-noise interaction is strong. In particular, two effects are evident: a shrinkage of the noise pdf along the radial direction, and a stretching and bending of the pdf around the origin. The first effect, corresponding to a reduction of the in-phase noise component a, is correctly predicted both by the RP and CRLP model, while the second effect, that is related to the presence of a strong phase noise, is correctly predicted only by the CRLP model. In this sense, the CRLP model gives a unified treatment of the parametric gain and nonlinear phase-noise effects. The agreement of the CRLP model with simulations is excellent for small perturbations, as evidenced by the inner contour line, and remains good even for large perturbations, as evidenced by the outer contour lines.

The nonlinear perturbation terms that are neglected in the linearization of the CRLP are responsible for the discrepancy between MMC and CRLP on the tips of the outer contour lines. This phase discrepancy is only observed for perturbations that are even larger than the signal itself, and are not expected to be relevant in amplitude-modulated systems. On the other hand, the RP model greatly overestimates the quadrature component b, that contributes to increasing the signal amplitude, and it does not predict the conversion of amplitude noise into phase noise.

Fig. 5(b) reports the pdf of the electrical signal after a standard OOK receiver. In this case, the CW power is $P_0 = 10\,\mathrm{mW}$, the noise PSD is $N_0 = 8 \cdot 10^{-15}\,\mathrm{W/Hz}$, and the fiber has an anomalous dispersion $D = 17\,\mathrm{ps/(nm \cdot km)}$ (a typical value for standard single-mode fibers). After propagation, the noisy optical signal is filtered by a band-pass Gaussian filter with a 3-dB bandwidth of 20 GHz, photodetected, and filtered again by a low-pass fifth-order Bessel filter with a 3-dB bandwidth of 7.5 GHz. In this case, taking the MMC simulations as a reference, parametric gain causes a strong increase of the pdf with respect to the AWGN model. This behavior, leading to a strong performance degradation in OOK systems, is accurately predicted by the CRLP model, but is not by the RP model, which instead predicts a performance improvement.

6 - Discussion and conclusions

The propagation of light in optical fibers is governed by the nonlinear Schrödinger equation (NLSE). In high-capacity and long-distance fiber-optic systems, both Kerr nonlinearity and GVD play a determinant role and affect system performance. Since they act together and are distributed along the link, it is hard to find a simple channel model and the system analysis must start from the NLSE itself.

In particular, two different problems should be considered, one being deterministic and the other stochastic. In this paper, we have given a general overview of the most common numerical and analytical approaches to both problems, with a special attention to the approaches based on perturbation theory.

As regards the deterministic problem, beside the well-known and widely adopted SSFM, we have presented and compared the RP and LP approaches. Starting from an integral expression of the NLSE, we have derived two alternative recursive expressions for the RP and LP methods that converge to the solution of the NLSE, the last one showing a significantly faster convergence.

As regards the stochastic problem, after a short discussion about the use of Monte Carlo methods, we have reviewed different approaches based on perturbation theory — the continuous wave (CW) approximation, the covariance matrix method (CMM), and the combined regular-logarithmic perturbation (CRLP) — and compared their accuracy, showing a good agreement between CRLP and simulation.

Despite the significant effort spent by the scientific community on this subject, several issues are still open to investigation. Concerning the deterministic problem, the accuracy of the SSFM is satisfactory for all telecom applications, and its computational efficiency is significantly higher than other numerical methods based on finite differences. However, for large-size problems (multi-span links and WDM systems), and mostly when the deterministic propagation must be repeated many times — as in the statistical approach to the stochastic problem — computational efficiency is still a big issue.

A possible approach worth further investigation is the LP one described in Section 4, for instance in order to find more efficient quadrature rules or analytic approximations for the integrals in (20). Concerning the stochastic problem, only MC methods give a general and accurate approach for any system, but they have a high computational cost and are practically unfeasible for complex systems. Reasonable approximations can be obtained by using analytical or semi-analytical methods based on perturbation theory, such as CMM or CRLP, even though they have some limitations. Future works include the extension of the CRLP method to modulated signals, as done in the CMM for instance, the inclusion of XPM and FWM from adjacent WDM channels, and the application to different modulation formats or

detection strategies, where both the phase and amplitude of the output optical signal are relevant. Finally, an interesting point to be investigated is the application of inverse scattering to the deterministic or stochastic problem in practical systems, including attenuation and dispersion compensation.

References

[1] G. P. Agrawal, *Nonlinear Fiber Optics*, 3rd ed., Academic Press, San Diego, CA 2001.

[2] G. Bellotti, M. Varani, C. Francia and A. Bononi, *Intensity distortion induced by cross-phase modulation and chromatic dispersion in optical fiber transmissions with dispersion compensation*, IEEE Photon. Technol. Lett. **10** (1998), 1745-1747.

[3] G. Bosco, A. Carena, V. Curri, R. Gaudino, P. Poggiolini and S. Benedetto, *Suppression of spurious tones induced by the split-step method in fiber systems simulation*, IEEE Photon. Technol. Lett. **12** (2000), 489-491.

[4] G. Bosco, A. Carena, V. Curri, R. Gaudino, P. Poggiolini and S. Benedetto, *A novel analytical approach to the evaluation of the impact of fiber parametric gain on the bit error rate*, IEEE Trans. Commun. **49** (2001), 2154-2163.

[5] A. Carena, V. Curri, R. Gaudino, P. Poggiolini and S. Benedetto, *New analytical results on fiber parametric gain and its effects on ASE noise*, IEEE Photon. Technol. Lett. **9** (1997), 535-537.

[6] A. B. Carlson, *Communication Sytems*, 3rd ed., McGraw Hill, New York 1986.

[7] A. V. T. Cartaxo, *Cross-phase modulation in intensity modulation direct detection WDM systems with multiple optical amplifiers and dispersion compensators*, J. Lightwave Technol. **17** (1999), 178-190.

[8] A. V. T. Cartaxo, *Small-signal analysis for nonlinear and dispersive optical fibres, and its application to design of dispersion supported transmission systems with optical dispersion compensation*, IEE Proc. Optoelectronics **146** (1999), 213-222.

[9] E. Ciaramella and E. Forestieri, *Analytical approximation of nonlinear distortions*, IEEE Photon. Technol. Lett. **17** (2005), 91-93.

[10] J. A. Fleck, J. R. Morris and M. D. Feit, *Time dependent propagation of high energy laser beams through the atmosphere*, Appl. Phys. **10** (1976), 129-160.

[11] E. Forestieri, *Evaluating the error probability in lightwave systems with chromatic dispersion, arbitrary pulse shape and pre- and postdetection filtering*, J. Lightwave Technol. **18** (2000), 1493-1503.

[12] C. Francia, *Constant step-size analysis in numerical simulation for correct four-wave-mixing power evaluation in optical fiber transmission systems*, IEEE Photon. Technol. Lett. **11** (1999), 69-71.

[13] L. Gerardi, M. Secondini and E. Forestieri, *Pattern perturbation method for multicanonical Monte Carlo simulations in optical Communications*, IEEE Photon. Technol. Lett. **19** (2007), 1934-1936.

[14] S. W. GOLOMB, *Shift register sequences*, Holden-Day, San Francisco 1967.

[15] J. P. GORDON and L. F. MOLLENAUER, *Phase noise in photonic communications systems using linear amplifiers*, Opt. Lett. **15** (1990), 1351-1353.

[16] R. H. HARDIN and F. D. TAPPERT, *Applications of the split-step Fourier method to the numerical solution of nonlinear and variable coefficient wave equations*, SIAM Rev. Chronicle **15** (1973), p. 423.

[17] A. HASEGAWA and F. TAPPERT, *Transmission of stationary nonlinear optical pulses in dispersive dielectric fibers. I. Anomalous dispersion*, Appl. Phys. Lett. **23** (1973), 142-144.

[18] C. W. HELSTROM and J. A. RITCEY, *Evaluating radar detection probabilities by steepest descent integration*, IEEE Trans. Aerospace Electron. Syst. **20** (1984), 624-634.

[19] K.-P. HO, *Impact of nonlinear phase noise to DPSK signals: a comparison of different models*, IEEE Photon. Technol. Lett. **16** (2004), 1403-1405.

[20] K.-P. HO and H.-C. WANG, *Cross-phase modulation-induced crosstalk for RZ-DPSK signals in dispersive transmission systems*, J. Lightwave Technol. **24** (2006), 396-403.

[21] R. HOLZLÖHNER, V. S. GRIGORYAN, C. R. MENYUK and W. L. KATH, *Accurate calculation of eye diagrams and bit error rates in optical transmission systems using linearization*, J. Lightwave Technol. **20** (2002), 389-400.

[22] R. HOLZLÖHNER and C. R. MENYUK, *Use of multicanonical Monte Carlo simulations to obtain accurate bit error rates in optical communications systems*, Opt. Lett. **28** (2003), 1894-1896.

[23] R. HOLZLÖHNER, C. R. MENYUK, W. L. KATH and V. S. GRIGORYAN, *A covariance matrix method to compute bit error rates in a highly nonlinear dispersion-managed soliton system*, IEEE Photon. Technol. Lett. **15** (2003), 688-690.

[24] R. HUI, M. O'SULLIVAN, A. ROBINSON and M. TAYLOR, *Modulation instability and its impact in multispan optical amplified IMDD systems: theory and experiments*, J. Lightwave Technol. **15** (1997), 1071-1081.

[25] M. KAC and A. J. F. SIEGERT, *On the theory of noise in radio receivers with square law detectors*, J. Appl. Phys. **18** (1947), 383-397.

[26] M. KARLSSON, *Modulational instability in lossy optical fibers*, J. Opt. Soc. Amer. B **12** (1995), 2071-2077.

[27] J.-S. LEE and C.-S. SHIM, *Bit-error-rate analysis of optically preamplified receivers using an eigenfunction expansion method in optical frequency domain*, J. Lightwave Technol. **12** (1994), 1224-1229.

[28] H. LOUCHET, A. HODŽIĆ, K. PETERMANN, A. ROBINSON and R. EPWORTH, *Analytical model for the design of multispan DWDM transmission systems*, IEEE Photon. Technol. Lett. **17** (2005), 247-249.

[29] A. MECOZZI, *Limits to long-haul coherent transmission set by the kerr nonlinearity and noise of the in-line amplifiers*, J. Lightwave Technol. **12** (1994), 1993-2000.

[30] A. PAPOULIS, *Probability, random variables, and stochastic processes*, 3rd ed., McGraw-Hill, New York 1991.

[31] J. G. PROAKIS, *Digital Communications*,4th ed., McGraw-Hill, New York 2001.

[32] M. SECONDINI, E. FORESTIERI and C. R. MENYUK, *A combined regular-logarith-*

mic perturbation method for signal-noise interaction in amplified optical systems, to be published.

[33] M. SECONDINI, E. FORESTIERI and C. R. MENYUK, *A novel perturbation method for signal-noise interaction in nonlinear dispersive fibers*, in Proc. OFC 2006, March 2006, paper OThD3.

[34] P. SERENA, A. BONONI, J.-C. ANTONA and S. BIGO, *Parametric gain in the strongly nonlinear regime and its impact on 10-Gb/s NRZ systems with forward-error correction*, J. Lightwave Technol. **23** (2005), 2352-2363.

[35] P. SERENA, A. ORLANDINI and A. BONONI, *Parametric-gain approach to the analysis of single-channel DPSK/DQPSK systems with nonlinear phase noise*, J. Lightwave Technol. **24** (2006), 2026-2037.

[36] O. V. SINKIN, V. S. GRIGORYAN and C. R. MENYUK, *Accurate probabilistic treatment of bit-pattern-dependent nonlinear distortions in BER calculations for WDM RZ systems*, J. Lightwave Technol. **25** (2007), 2959-2968.

[37] O. V. SINKIN, R. HOLZLÖHNER, J. ZWECK and C. R. MENYUK, *Optimization of the split-step Fourier method in modeling optical-fiber communications systems*, J. Lightwave Technol. **21** (2003), 61-68.

[38] P. J. SMITH, M. SHAFI and H. GAO, *Quick simulation: a review of importance sampling techniques in communications systems*, IEEE J. Sel. Areas Commun. **15** (1997), 597-613.

[39] T. R. TAHA and M. J. ABLOWITZ, *Analytical and numerical aspects of certain nonlinear evolution equations. II. Numerical, nonlinear Schrödinger equation*, J. Computat. Phys. **55** (1984), 203-230.

[40] S. TEN, K. M. ENNSER, J. M. GROCHOCINSKI, S. P. BURTSEV and V. L. DASILVA, *Comparison of four-wave mixing and cross phase modulation penalties in dense WDM systems*, in Proc. OFC/IOOC'99 **3** (1999), paper ThC4-1, 43-45.

[41] A. VANNUCCI, P. SERENA and A. BONONI, *The RP method: a new tool for the iterative solution of the nonlinear Schrödinger equation*, J. Lightwave Technol. **20** (2002), 1102-1112.

[42] V. E. ZAKHAROV and A. B. SHABAT, *Exact theory of two-dimensional self-focusing and one-dimensional self-modulation of waves in nonlinear media*, Sov. Phys. JETP **34** (1972), 62-69.

Abstract

We review some numerical and analytical approaches to the solution of the nonlinear Schrödinger equation for the propagation of optical signals in fiber-optic communication systems. As regards the propagation of deterministic signals, we derive two alternative recursive expression, based on a regular perturbation and a logarithmic perturbation expansion, that, starting from the linear solution, converge to the exact solution of the equation. As regards the propagation of stochastic processes, we review different approaches based on perturbation theory, namely, the continuous wave approximation, the covariance matrix method, and the combined regular-logarithmic perturbation. We discuss accuracy, complexity, and limitations of all the methods and compare them with numerical simulations.

* * *